Multi-omic spatial data integration resolves immunometabolic heterogeneity associated with Nivolumab response in non-small cell lung cancer (NSCLC) patients

Raymond Yan[1], Shannon Quinn[1], Brian Falkenstein[1], James Monkman[2], Kenneth O'Bryne[2,3], A. Burak Tosun, S Chakra Chennubhotla[1,4], **Filippo Pullara[1]**, Arutha Kulasinghe[2]

[1]PredxBio, Inc., 100 S. Jackson Ave., Pittsburgh, PA USA 15202; [2]Frazer Institute, Faculty of Medicine, The University of Queensland, Brisbane, Queensland, Australia; [3] Princess Alexandra Hospital, Woolloongabba, Queensland 4102, Australia; [4] Dept. of Computational and Systems Biology, University of Pittsburgh, Pittsburgh, USA

Background

- Non-Small Cell Lung Cancer (NSCLC) accounts for most lung cancers and has a poor 5-year survival.
- Spatial intratumoral heterogeneity of the tumor microenvironment (TME) is not well-understood for NSCLC contributing to ineffective immunotherapies (ICI).
- Advanced multiplex techniques in both spatial proteomics and spatial transcriptomics are currently used for generating novel hypotheses on immunometabolic pathway crosstalk, developing predictive spatial biomarkers and targeting metabolic determinants of immunotherapy response.

Methods

- Study performed on a retrospective cohort of *second-line nivolumab-treated* NSCLC tissue cores – **N = 28 (responders = 10/non-responders = 18)** [1].
- Cohort was profiled using a **custom 44-plex mIF panel** [1] (incl. functional/metabolic markers) with the Phenocycler Fusion platform (Akoya Biosciences) and ROI-based bulk transcriptomics (Nanostring GeoMx DSP, 1812 curated genes) and co-registered through alignment of DAPI.
- We applied **SpaceIQ™** [2,3], an unbiased spatial analytics and explainable AI platform, for mIF markers-based cell segmentation & unbiased cell typing on entire tissue cores.
- Cell type-specific gene expression profiles were estimated through RNA deconvolution on 147 differentially expressed genes.
- Outcome-specific microdomains were then derived using pointwise-mutual information (PMI) [4] on the core-based cell types.
- Microdomain-guided gene pathway enrichment and significant proteomic biomarker pathways were annotated based on Ingenuity Pathway Analysis and STRING database, respectively.

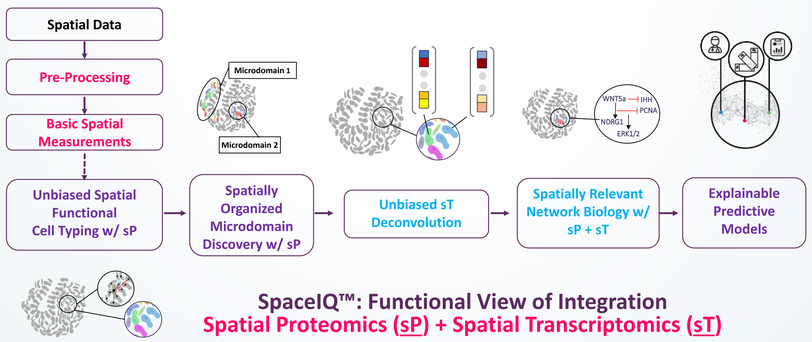

SpaceIQ™: Functional View of Integration
Spatial Proteomics (sP) + Spatial Transcriptomics (sT)

Results

- Microdomain discovery from core-based cell types resulted in a distinct set of enriched pathways from multi-omic integration of mIF and DSP bulk RNA data.
- Predictive performance between the two approaches using spatial transcriptomics and spatial proteomics yielded comparable performances.
- ROI-based microdomains implicated lipid metabolism (p=0.02), fatty acid oxidation (p=0.04), Notch Signaling (p=0.01), and NK-mediated activity (p=0.06) in nivolumab-treated response.
- Core-based microdomains were enriched for cell differentiation (p<0.01), mitochondrial metabolism / TCA (p=0.01), and lymphocyte trafficking (p=0.08).

Contact:
- **Chakra Chennubhotla, PhD**
  chakra@predxbio.com **(or)**
  chakracs@pitt.edu
- **Arutha Kulasignhe, PhD**
  arutha.kulasinghe@uq.edu.au

Read SpaceIQ White Paper

Follow us on LinkedIn

PUBLICATIONS

Unbiased Cell Typing Extracts Numerically Stable, Spatially Distinct and Biologically Interpretable Recursive Cell Types

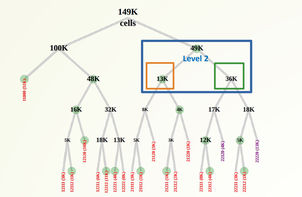

- Green circles denote distinct sub-populations based on goodness-of-cluster
- Red cell types denote a sub- population with a distinct parent not from level 1
- Purple cell types denote cell population that derive level 1 distinctiveness

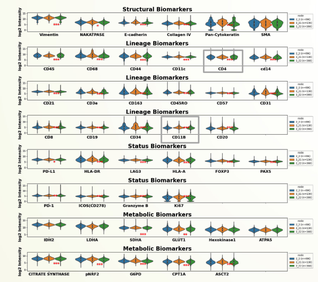

Differential biomarker intensity distributions for level 2 sub-populations (orange and green) from *n* = 100K cells (blue) (*** indicates statistically significant differences).

Perform Unbiased sT Deconvolution w/ Functional Cell Types Derived from sP

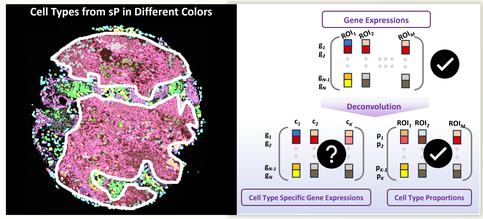

Cell Types	Cell Annotations	Kendall Tau Corr. (max)
11000	CD1c-positive_myeloid_dendritic_cell , myeloid_cell , non-classical_monocyte , pericyte , smooth_muscle_cell	0.37
12111	stromal_cell	0.29
12112	mesothelial_cell , stromal_cell , type_II_pneumocyte	0.32
12120	mesothelial_cell , smooth_muscle_cell , stromal_cell , type_II_pneumocyte	0.31
12212	CD1c-positive_myeloid_dendritic_cell , myeloid_cell , stromal_cell , type_II_pneumocyte	0.32
12221	mesothelial_cell , pericyte , type_II_pneumocyte	0.31
12222	mesothelial_cell , stromal_cell , type_II_pneumocyte	0.31
21111	CD1c-positive_myeloid_dendritic_cell , capillary_endothelial_cell , myeloid_cell , non-classical_monocyte , pericyte , stromal_cell	0.40
21112	mesothelial_cell , stromal_cell , type_II_pneumocyte	0.31
21211	mesothelial_cell	0.27
21212	CD1c-positive_myeloid_dendritic_cell , myeloid_cell , non-classical_monocyte , pericyte	0.32
22111	CD1c-positive_myeloid_dendritic_cell , myeloid_cell , non-classical_monocyte , pericyte	0.30
22112	mesothelial_cell , pericyte , stromal_cell , type_II_pneumocyte	0.30
22211	CD1c-positive_myeloid_dendritic_cell , myeloid_cell , non-classical_monocyte , pericyte , regulatory_T_cell	0.38
22212	CD1c-positive_myeloid_dendritic_cell , non-classical_monocyte , pericyte	0.36
22220	CD1c-positive_myeloid_dendritic_cell , myeloid_cell , non-classical_monocyte , pericyte , smooth_muscle_cell	0.37

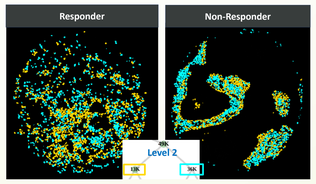

Spatial distribution of the discriminating biomarkers for level 2 – CD118 (cyan) and CD4 (yellow) on a responder and a non-responder core.

Unbiased Cell Typing Reveals Differential Metabolic Activity in Tumor (Stroma) Cell Types in Non-Responders (Responders)

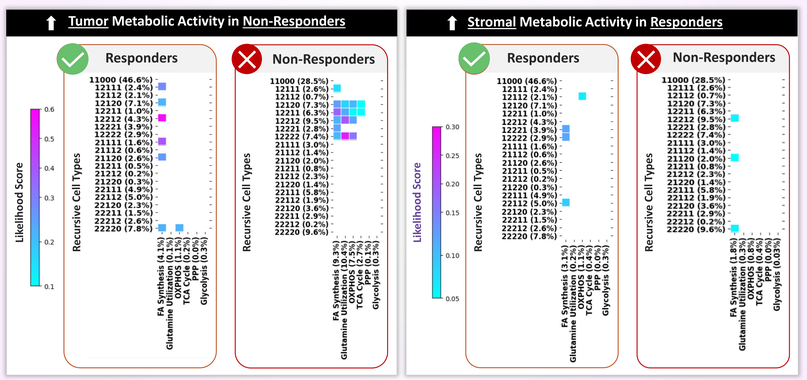

Conclusions

- The SpaceIQ platform enables **integration of mIF and RNA expression** data from Nivolumab-treated NSCLC tissue samples to discover microdomains associated with treatment response.
- **Microdomains associated with treatment response** suggest the role of canonical metabolic programs and immune cell differentiation/migration in improved outcomes.
- Further investigation in the immuno-metabolic states within the TME will lead to more **effective ICI treatment strategies for NSCLC**.

Microdomains Emerge as Spatial Networks of Immuno-Metabolic Cell Types

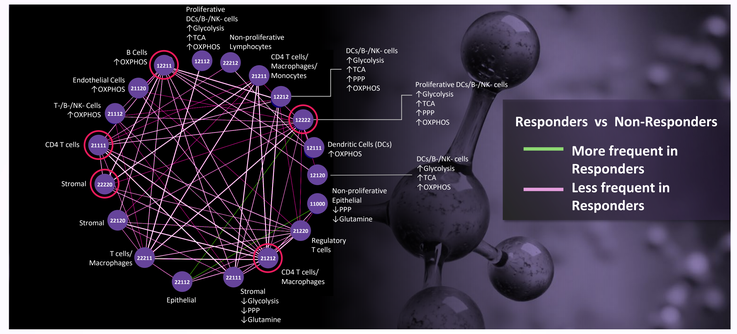

Microdomain	Cell Types	Proteomic Mean AUC (SD)
1	'11000', '21212', '21220', '22112'	0.75 (0.12)
2	'12111', '12211', '12222'	0.75 (0.15)
3	'12120', '12211', '12222'	0.84 (0.12)
4	'12211', '12212', '12222', '21111', '21212'	0.73 (0.14)
5	'12211', '12212', '12222', '21112', '21212'	0.70 (0.13)
6	'12211', '12212', '21111', '21212', '22111'	0.67 (0.13)
7	'12211', '12212', '21112', '21212', '22111'	0.69 (0.12)
8	'12211', '12222', '21111', '21212', '22211'	0.75 (0.12)
9	'12211', '12222', '21111', '21212', '22220'	0.84 (0.12)
10	'12211', '12222', '21112', '21212', '22211'	0.72 (0.13)
11	'12211', '12222', '21120', '21212'	0.72 (0.13)
12	'12211', '12222', '21212', '22120', '22211'	0.72 (0.12)
13	'12211', '21212', '22111', '22120'	0.68 (0.13)

Microdomain	Cell Types	Proteomic Mean AUC (SD)
14	'12212', '12222', '21111', '21212', '21220'	0.83 (0.12)
15	'12212', '21111', '21211', '21212', '22111'	0.67 (0.11)
16	'12212', '21111', '21212', '21220', '22111'	0.66 (0.11)
17	'12222', '21111', '21212', '21220', '22211'	0.76 (0.13)
18	'12222', '21111', '21212', '21220', '22220'	0.78 (0.10)
19	'12222', '21120', '21212', '21220'	0.73 (0.12)
20	'12222', '21212', '21220', '22112', '22211'	0.79 (0.13)
21	'12222', '21212', '21220', '22120', '22211'	0.79 (0.13)
22	'21111', '21211', '21212', '22211'	0.64 (0.12)
23	'21111', '21211', '21212', '22220'	0.74 (0.14)
24	'21211', '21212', '22111', '22120'	0.62 (0.11)
25	'21211', '21212', '22120', '22211'	0.61 (0.10)
26	'21212', '21220', '22111', '22120'	0.67 (0.13)

Microdomain	Cell Types	Proteomic Mean AUC (SD)	Genomic Mean AUC (SD)	Proteomic+Genomic Mean AUC (SD)
3	'12120', '12211', '12222'	0.84 (0.12)	0.85 (0.12)	0.86 (0.14)
4	'12211', '12212', '12222', '21111', '21212'	0.73 (0.14)	0.81 (0.17)	0.70 (0.16)
8	'12211', '12222', '21111', '21212', '22211'	0.75 (0.12)	0.75 (0.22)	0.71 (0.23)
11	'12211', '12222', '21120', '21212'	0.72 (0.13)	0.79 (0.31)	0.69 (0.31)
22	'21111', '21211', '21212', '22211'	0.64 (0.12)	0.7 (0.27)	0.6 (0.26)

Microdomains are Spatially Distinct Catabolic and Anabolic Programs that Predict ICI Response

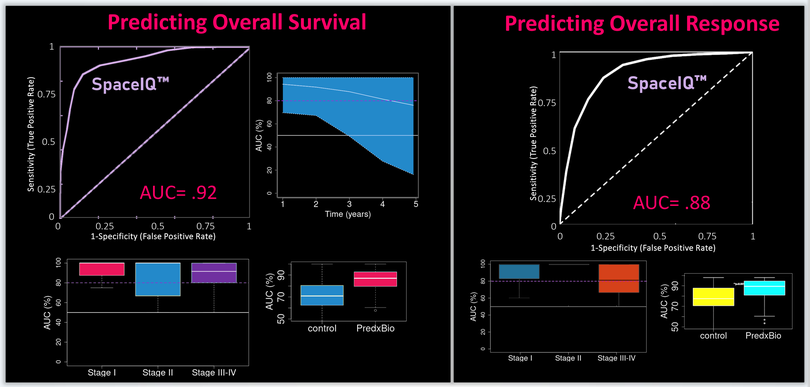

Microdomains are highly predictive of overall survival and response. Some microdomains are spatially anchored around tumor cells with upregulated TCA cycle and oxidative phosphorylation (OXPHOS) with additional NK cells and dendritic cells along with upregulated PPP. Some microdomains capture spatially distinct metabolic programs relating to catabolic (energy utilization) and anabolic (cellular biogenesis) pathways.

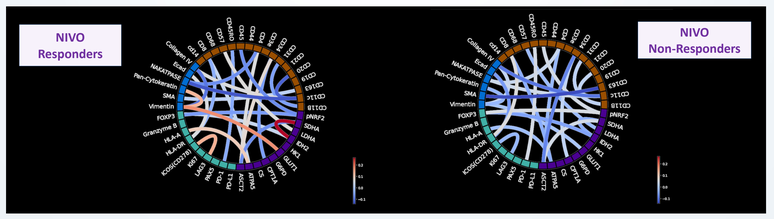

References [1]Monkman et al Immunology, 2023; [2]Uttam, S, et al Nat. Comm., 2020; [3]Furman SA, Cell. Rep. Met., 2021; [4]Spagnolo D et al, JPI, 2016